

Gaussian Belief Trees for Chance Constrained Asymptotically Optimal Motion Planning

Qi Heng Ho, Zachary N. Sunberg, and Morteza Lahijanian

Abstract—In this paper, we address the problem of sampling-based motion planning under motion and measurement uncertainty with probabilistic guarantees. We generalize traditional sampling-based, tree-based motion planning algorithms for deterministic systems and propose belief- \mathcal{A} , a framework that extends any kinodynamical tree-based planner to the belief space for linear (or linearizable) systems. We introduce appropriate sampling techniques and distance metrics for the belief space that preserve the probabilistic completeness and asymptotic optimality properties of the underlying planner. We demonstrate the efficacy of our approach for finding safe low-cost paths efficiently and asymptotically optimally in simulation, for both holonomic and non-holonomic systems.

I. INTRODUCTION

In recent years, sampling-based algorithms (e.g., [1]–[5]) have emerged as powerful motion planning tools as they can search high dimensional spaces very efficiently and find solutions to complex problems quickly. They have enabled many applications such as self-driving cars, surgical robots, and autonomous UAVs. The majority of such planners assume perfect state information. However, an inseparable aspect of robotics is uncertainty in motion (e.g., due to modeling inaccuracies) and observation (e.g., due to noisy sensors). This gap is especially significant when measurement uncertainty makes it difficult to find efficient paths while obeying safety constraints. This work focuses on this gap and aims to develop a general framework for adapting existing sampling-based algorithms to plan for uncertain systems with safety and optimality guarantees.

Consider a UAV equipped with a GPS receiver navigating under a canopy in a forest for a search and rescue task. The ability of the UAV to estimate its state is dependent on where it is in the forest, as some regions may have improved GPS accuracy or connectivity than others. To plan safe paths under dynamics and sensor noise, the robot has to trade off between visiting such regions or taking the shortest path to the goal location. Explicitly and intelligently accounting for both motion and measurement uncertainty is necessary to improve the quality and safety of motion plans.

In its most general form, planning under uncertainty can be formulated as a Partially Observable Markov Decision Process (POMDP) [6]. POMDP solvers attempt to find an optimal policy in the belief space, which is the space of all possible probability distributions over the state space. Unfortunately, this problem is computationally intractable due

to the curses of dimensionality and history [7]. Methods for approximating POMDP solutions for motion planning over continuous state, control, and observation spaces have been proposed, e.g., [8], [9]. However, they do not perform well especially when the action (control) space is large, which is a characteristic of robotic systems. Another drawback is the lack of guarantees in these solutions.

In recent years, sampling-based algorithms have been extended to account for motion uncertainty with probabilistic guarantees, e.g., [10]–[18]. Specifically, the chance-constrained tree-based planners have shown to be efficient, and hence, employed in unknown environments via iterative planning [10]–[12], [15]. A few studies extend those frameworks to systems with measurement uncertainty [19]–[22]. For instance, in [21], [22], maximum-likelihood observations are used to approximate solutions. While that approach works well in many cases, it lacks safety guarantees. Work [23] proposes an alternative approach that provides chance-constrained guarantees by combining optimal control and state estimation with sampling-based graphs. The method finds an optimal trajectory through the belief space by constructing a graph of trajectories in the state space and enumerating all possible uncertainty levels for these trajectories in the belief space. That planner is asymptotically optimal and has probabilistic safety guarantees, but it suffers from large computation times.

To mitigate that issue, work [24] extended the method by using branch-and-bound pruning, which leads to linear computation speedups. However, it also modifies the cost function of the problem to include uncertainty, which may affect the optimality of its solutions with respect to the original cost function.

In this paper, we generalize tree-based motion planning to obtain a belief planning framework for linear (or linearizable) systems with both motion and observation uncertainty. This framework, called belief- \mathcal{A} , enables the use of any kinodynamical planner \mathcal{A} for belief space motion planning. Belief- \mathcal{A} provides chance constraint guarantees, and preserves the probabilistic completeness and asymptotic optimality properties of the underlying planner as well as its computational efficiency. This is achieved by utilizing appropriate sampling techniques and distance metrics in the belief space.

Specifically, our contributions are (i) a general method to extend state space sampling-based tree search algorithms directly to the Gaussian belief space, (ii) a method to uniformly sample in the belief space, (iii) a way to heuristically bias sampling towards low uncertainty belief states, and (iv) the use of the 2-Wasserstein metric for distance computation

This work was supported by the University of Colorado Boulder.

Authors are with the department of Aerospace Engineering Sciences at the University of Colorado Boulder, CO, USA {*firstname.lastname*}@colorado.edu

between beliefs. We show the efficacy of our framework through benchmarking and numerical characterization in several scenarios that highlight the relative strengths of different aspects of our framework. The results indicate that our method performs much faster (up to 50 times speedup) compared to prior belief space tree search methods while still having asymptotically near-optimal guarantees, allowing for safe and efficient planning. As a by-product of the computational speedups, we also show the ability of our planner to conduct online re-planning when knowledge of the environment changes.

II. PROBLEM FORMULATION

We are interested in motion planning for a robotic system with uncertainty in both motion and observation (measurement) with safety guarantees. We assume the robot evolves in a bounded workspace (\mathbb{R}^2 or \mathbb{R}^3) with obstacles according to linear or linearizable dynamics and a measurement model that can change in different parts of the environment, e.g., GPS signal may be available only in parts of the environment. Below, we formalize this problem.

Let $\mathcal{X} \subset \mathbb{R}^n$ and $\mathcal{U} \subset \mathbb{R}^m$ be the state and control spaces, respectively. Then, the robot model is given by:

$$\begin{aligned} x_k &= Ax_{k-1} + Bu_{k-1} + w_k, & w_k &\sim \mathcal{N}(0, Q), \\ z_k &= Cx_k + v_k(x_k), & v_k(x_k) &\sim \mathcal{N}(0, R(x_k)), \end{aligned} \quad (1)$$

where $x_k \in \mathcal{X}$ is the state, $u_k \in \mathcal{U}$ is the input, $z_k \in \mathbb{R}^p$ is the measurement. Furthermore, matrices $A \in \mathbb{R}^{n \times n}$, $B \in \mathbb{R}^{n \times m}$, and $C \in \mathbb{R}^{p \times n}$. Terms w_k and v_k are i.i.d white Gaussian noise with zero mean and Q and $R(x_k)$ covariance matrices, respectively. Note that a unique aspect of this robot model is that the measurement noise (covariance matrix) is a function of the state, representing, e.g., various types of measurement regions in the environment.

We assume the system's dynamics are fully controllable and observable, and the noise covariance matrices Q and $R(x_k)$ are non-degenerate. For presentation simplicity, we focus on the time-invariant system in (1), but the formulation can be easily extended to time-varying systems.

The evolution of the robotic system in (1) can be described by a discrete-time Gaussian Markov process. The robot state x_k at each time step can be described as a Gaussian distribution $b_k = \mathcal{N}(\hat{x}_k, \Sigma_k)$, where $b_k \in \mathcal{B}$ is referred to as the belief of the robot state, \mathcal{B} is the *belief space* of the robot, and \hat{x}_k and Σ_k are the state mean and covariance matrix, respectively. In this work, we search for a motion plan characterized by a sequence of nominal control inputs and the nominal trajectory that they produce in the absence of uncertainty, along with a linear feedback controller that seeks to follow this trajectory using online state estimate \hat{x}_k .

Let $\tilde{U}^{0,t} = (\tilde{u}_0, \tilde{u}_1, \dots, \tilde{u}_{t-1})$ be a sequence of control inputs. Given an initial state x_0 and nominal system dynamics $\tilde{x}_{k+1} = A\tilde{x}_k + B\tilde{u}_k$, a nominal trajectory $\tilde{X}^{x_0, x_t} = (\tilde{x}_0, \tilde{x}_1, \dots, \tilde{x}_t)$ is obtained. This motion plan is then executed online via a stabilizing controller given online state estimates \hat{x}_k . This gives us the following online control input

$$u_k = \tilde{u}_{k-1} - K(\hat{x}_k - \tilde{x}_k), \quad (2)$$

where K is the closed loop gain. For simplicity, we use a fixed controller gain, but a variable gain can also be used. We refer to (\tilde{U}, \tilde{X}) as a *motion plan* for System (1).

Let $\mathcal{X}_{obs}, \mathcal{X}_{goal} \subset \mathcal{X}$ represent the state space obstacles and the goal region respectively. For robot state x_k and its belief b_k , the probability of the robot being in \mathcal{X}_i , where $i \in \{obs, goal\}$, is given by

$$p(x_k \in \mathcal{X}_i) = \int_{\mathcal{X}_i} b_k(y) dy. \quad (3)$$

Furthermore, consider a stage cost function $J : \mathcal{X} \rightarrow \mathbb{R}^+$ that is monotonic and Lipschitz continuous. Given safety probability P_{safe} , we desire an optimal motion plan that minimizes total cost given by J and whose probability of collision at every time step and probability of not ending in goal are upper bounded by P_{safe} . The formal statement of this problem is as follows.

Problem 1. *Given a robot with noisy dynamics and measurements as in (1), a set of state space obstacles \mathcal{X}_{obs} , a goal region \mathcal{X}_{goal} , a Lipschitz continuous cost function $J : \mathcal{X} \rightarrow \mathbb{R}^+$, and a safety probability bound P_{safe} , find a motion plan $(\tilde{U}, \tilde{X})^*$ as a pair of sequence of nominal controls $\tilde{U} = (\tilde{u}_0, \dots, \tilde{u}_{T-1})$ for some $T \geq 1$ and its resulting nominal trajectory $\tilde{X} = (\tilde{x}_0, \dots, \tilde{x}_T)$ that minimizes the expected total cost,*

$$(\tilde{U}, \tilde{X})^* = \arg \min_{(\tilde{U}, \tilde{X})} \mathbb{E} \left[\sum_{t=0}^T J(x_t) \right], \quad (4)$$

subject to, when executed via controller in (2), the probabilities of collision with \mathcal{X}_{obs} and not ending in \mathcal{X}_{goal} are bounded by P_{safe} , i.e.,

$$p(x_t \in \mathcal{X}_{obs}) < P_{safe}, \quad \forall t \in [0, T], \quad (5)$$

$$p(x_T \notin \mathcal{X}_{goal}) < P_{safe}. \quad (6)$$

To solve this optimal motion planning problem, we aim to design an algorithm that is asymptotically optimal, i.e. the probability of finding the optimal solution converges to 1 as the number of iterations approaches infinity. For our applications of interest, asymptotic near-optimality (i.e., the solution converges to within an approximation factor ϵ of the optimal solution) is sufficient, but our proposed framework is not limited to asymptotic near-optimality.

III. PRELIMINARIES

Here, we introduce the preliminaries required to introduce our solution to the above problem.

A. Asymptotically-Optimal Tree Search Planners

Typical single query sampling-based tree search algorithms construct a tree in the search space. For kinodynamic systems without any uncertainty, this search space is the state space. In this work, we aim to develop a method to transform such existing planners into belief space planners that solve Problem 1. To this end, we first present an overview of such planners.

Algorithm 1 shows a generic form of an asymptotically optimal tree-based planner for kinodynamical systems. It takes state space \mathcal{X} , input space \mathcal{U} , goal region \mathcal{X}_{goal} , obstacle regions \mathcal{X}_{obs} , an initial state x_{init} , and a maximum planning time or iteration count (N) as input and returns a near-optimal solution, if one is found. Search is performed by growing a motion tree in which states and the connections between them are stored as nodes in \mathbb{V} and edges in \mathbb{E} , respectively. Note that the Prune subroutine is not mandatory for asymptotic optimality, but many asymptotically optimal planners, e.g., the Stable Sparse-RRT (SST) [25], utilize it.

Algorithm 1: Generic Asymptotically-Optimal Tree-based Planner $\mathcal{A}(\mathcal{X}, \mathcal{U}, \mathcal{X}_{goal}, \mathcal{X}_{obs}, x_{init}, N)$

Output: Valid Trajectory $x_{1:T}$ if one is found

```

1  $G = (\mathbb{V} \leftarrow \{x_{init}\}, \mathbb{E} \leftarrow \emptyset)$ 
2 for  $N$  iterations do
3    $x_{rand} \leftarrow \text{Sample}()$ 
4    $n_{select} \leftarrow \text{Select}(x_{rand})$ 
5    $n_{new} \leftarrow \text{Extend}(n_{selected})$ 
6   if  $\text{isValidPath}(n_{select}, n_{new})$  then
7      $\mathbb{V} \leftarrow \mathbb{V} \cup \{n_{new}\}$ 
8      $\mathbb{E} \leftarrow \mathbb{E} \cup \{\text{edge}(n_{select}, n_{new})\}$ 
9   Prune( $\mathbb{V}, \mathbb{E}$ )
10 return  $G = (\mathbb{V}, \mathbb{E})$ 

```

B. Propagation of Beliefs through Feedback Dynamics

Following [23], given a stabilizing feedback controller in (2) and online state estimate \hat{x}_k , the system closed-loop dynamics are

$$x_k = Ax_k + B(\hat{u}_{k-1} - K(\hat{x}_k - \check{x}_k)) + w_k. \quad (7)$$

The belief during planning is parameterized as

$$b_k = P(x_k) = \mathcal{N}(\check{x}_k, \Sigma_k^+ + \Lambda_k^+), \quad (8)$$

where Σ_k^+ is the covariance that represents the online state estimation error, and Λ_k^+ is the uncertainty over possible state estimates that could arise during execution and is a result of considering all possible measurements received. Σ_k^+ and Λ_k^+ can be computed recursively using the Kalman Filter:

$$\Sigma_k^- = A\Sigma_{k-1}^+A^T + Q, \quad (9)$$

$$L_k = \Sigma_k^- C^T (C\Sigma_k^- C^T + R(\hat{x}_k))^{-1}, \quad (10)$$

$$\Sigma_k^+ = \Sigma_k^- - L_k C \Sigma_k^-, \quad (11)$$

$$\Lambda_k^+ = (A - BK)\Lambda_{k-1}^+(A - BK)^T + L_k C \Sigma_k^-. \quad (12)$$

IV. GAUSSIAN BELIEF TREES

Here, we present our methodology for finding chance-constrained motion plans in the belief space to solve Problem 1. We present our framework in its general form, which can be used with any single-query state space tree-based motion planner with a structure similar to Algorithm 1. Instead of planning in the state space, we plan in the belief space \mathcal{B} , where $b \in \mathcal{B}$ is a Gaussian distribution as defined in (8). Vertices in the tree structure are now belief nodes, rather than state nodes.

As discussed in Section III-A and Algorithm 1, the main subroutines for tree search algorithms are the sample, select, extend, and validity checking. Below, we present methods for reformulating these functions for reasoning in the belief space. Specifically, we show how to sample directly in the belief space, and propose a method for heuristically biasing the sampling. Then, we present a belief space distance function for node selection through the use of a suitable distance metric for probability distributions. Finally, we present our approach to belief propagation and validity checking.

A. Sampling Strategy

Since our beliefs are Gaussian distributions, the Sample function must randomly sample the first moment (mean μ_s) and second moment (covariance matrix Σ_s).

1) *Sampling of first moment:* Similar to state space planning, we sample the mean of a belief from the state space, such that $\mu_s \in \mathcal{X}$. We also utilize a goal bias, in which we sample μ_s within the goal region with a probability p_{goal} , which yields faster convergence in practice [26].

2) *Sampling of covariance matrices:* The optimal sampling strategy for motion planning in Gaussian belief spaces is an open question, but it is crucial that the method for sampling covariance matrices completely samples the space of covariances for a problem environment in order to preserve probabilistic completeness of the state space version of the algorithm. We show how to uniformly sample the space of covariance matrices for a given environment.

We first observe that since Q and R are assumed to be non-degenerate, the covariance matrix of b_k is necessarily positive definite. Hence it is always diagonalizable, i.e., we can write $\Sigma_s = ODO^T$, where D is a $n \times n$ diagonal matrix whose diagonal elements consist of its non-negative eigenvalues and O is a $n \times n$ orthogonal matrix whose columns consist of its linearly independent real and orthonormal eigenvectors. Therefore, we can sample Gaussian covariance matrices by generating eigenvalues for D and an orthogonal matrix O of eigenvectors. To do this, we first uniformly sample eigenvalues λ_i from the interval $(0, \lambda_{i,max}]$ where $\lambda_{i,max}$ defines the maximum allowed eigenvalue for the i^{th} dimension. $\lambda_{i,max}$ depends on the environment. One method for setting $\lambda_{i,max}$ is to find the minimum $\lambda_i > \lambda_{i,max}$ such that forming a diagonal covariance matrix with λ_i as the i^{th} diagonal element and setting the rest of the diagonal elements as a small ϵ violates the chance constraint at every state in the state space.

Next, to uniformly sample random orthogonal matrices O , we first generate an $n \times n$ matrix M whose elements are independently sampled from a standard normal distribution (with mean 0 and standard deviation 1). The QR decomposition of M , i.e., $M = OR$, then provides a uniform distribution of an orthogonal matrix O [27]¹. Finally, we obtain our randomly sampled Gaussian covariance matrix by computing $\Sigma_s = ODO^T$.

¹Sampling elements of M with another distribution, e.g. uniform, still randomly samples an orthogonal matrix O , but not necessarily uniformly.

3) *Sampling bias*: To improve performance, we can exploit the intuition that low uncertainty beliefs result in reduced collision probability, which improves the chances of finding new valid edges and nodes. Additionally, since the problems we are interested in have an inherent tradeoff between motion plans that have lower cost and those that have higher cost but lead to lower uncertainty trajectories, this low uncertainty bias provides a way to prioritize lower uncertainty paths without explicitly considering it in the cost.

Therefore, with probability p_{bias} , we sample a fixed low eigenvalue $\lambda_{i,low}$ instead of uniformly in the interval $(0, \lambda_{i,max}]$. This effectively pulls the tree towards low uncertainty areas in the belief space, behavior empirically shown in our experiments to be advantageous, while still ensuring completeness. The optimum p_{bias} depends on the environment, where a high p_{bias} is useful for environments in which solution paths require low uncertainty but may slow down convergence if low uncertainty is not required. In the general case, p_{bias} should be set to a low value to ensure a more general coverage of the search space.

B. Belief Space Metric

A key component of many tree-based algorithms, such as RRT [2] and SST [25], is a distance metric to compute distances between nodes in the tree. This metric is used for near neighbor computations, to select which node to extend in the Select function, and for pruning. A good choice of distance metric can greatly affect exploration of the search space, planning time and path quality [28], [29].

In the Gaussian belief space, a typical state space distance metric such as Euclidean distance can still be used on the means of the belief nodes, but that is not ideal as they do not capture the uncertainty of the belief state. Instead, we use the Wasserstein distance [30], which is a metric on a space of probability measures. Intuitively, the Wasserstein metric is the amount of work required to move the probability mass of one distribution to another. For two non-degenerate Gaussian beliefs b_1 and b_2 with $b_i \sim N(\mu_i, \Sigma_i)$, with respect to the Euclidean norm on \mathbb{R}^n , the 2-Wasserstein distance is

$$D_{W_2}(b_1, b_2) = \|\mu_1 - \mu_2\|_2^2 + \text{Tr}(\Sigma_1 + \Sigma_2 - 2(\Sigma_1^{\frac{1}{2}}\Sigma_2\Sigma_1^{\frac{1}{2}})^{\frac{1}{2}}), \quad (13)$$

where $\text{Tr}(M)$ is the trace of M . Unlike other belief distance functions such as KL-divergence and LP-distance, the Wasserstein metric is a true metric in the belief space and has desirable properties for the preservation of asymptotic optimality of the state space algorithm (see Section V-A).

C. Extend/Propagate

After selecting a belief node, using the sampling method and distance metric described above, kinodynamic tree-search algorithms create a new node in the tree by extending the selected node using a computed nominal control input and random time duration. Given a belief node b , nominal control inputs \tilde{u} and a time duration, we propagate the belief to a new belief node b' using (8)-(12). The control inputs can

be computed by either repeatedly sampling the control space directly or sampling a state x_{sample} and applying a closed loop controller for a sampled time duration.

It is important to note that although the system is linear and controllable which implies that we can always compute a control input to steer a state node to any other state, steering between two Gaussian belief nodes involves not only steering the means from one belief to another, but propagation from one covariance to another. Even for a linear system, a solution for controlling an arbitrary Gaussian covariance to converge to another arbitrary covariance is not guaranteed to exist. Therefore, tree-search algorithms that rely on a steering function between two nodes, such as RRT*, cannot be readily extended to the belief space via our method.

D. Validity Checking

Validity checking in the state space involves deterministic collision checking, i.e. checking if $x \in \mathcal{X}_{obs}$. In the belief space, it involves computing the probability of collision $p(x) \in \mathcal{X}_{obs}$ in (3), which involves an integral. The exact evaluation of this integral over obstacles is not always computable, and numerical integration is computationally expensive. Efficient conservative approximations can be computed very quickly for convex polygonal obstacles using error functions as proposed in [11]. For non-convex obstacles, methods such as [12], [31] provide high accuracy at the cost of computation time.

V. ANALYSIS

A. Completeness and Optimality

The belief space extension inherits the probabilistic completeness and asymptotic (near)-optimality properties of the state space versions of the algorithms. The following theorems formalize these properties.

Theorem 1 (Completeness). *Algorithm belief-A is probabilistically complete for the stochastic system in (1) if A is probabilistically complete for the nominal system in (1) (without stochasticity).*

Proof Sketch. Probabilistic completeness for tree-search algorithms requires that the search space is completely sampled almost surely. The main relevant consequence of the change to the belief space is the difference in sampling of the search space and propagation dynamics. However, with the sampling method described in IV-A, beliefs are sampled uniformly, which implies the search space is completely sampled almost surely (the inclusion of the bias term does not change the result). Additionally, if the dynamics is Lipschitz continuous, the propagation method presented in the belief space is also Lipschitz continuous. Hence, Belief-A inherits the probabilistic completeness properties of A. \square

The use of the 2-Wasserstein metric makes the new belief space a proper metric space, and it is known that the 2-Wasserstein metric preserves the Lipschitz continuity of the cost function [29], [32].

Lemma 1. *Theorem in [29]. For any control input $u \in \mathcal{U}$, if the cost function in the state space is Lipschitz continuous in the state space, then the expected cost function in the belief space with the 2-Wasserstein metric is also Lipschitz continuous.*

Convergence guarantees for asymptotically (ϵ -)optimal sampling-based planners typically rely on Lipschitz continuity in the cost function [29]. This motivates the following theorem:

Theorem 2 (Optimality). *Belief- \mathcal{A} is asymptotically (ϵ -)optimal if algorithm \mathcal{A} is asymptotically (ϵ -)optimal under the conditions in Problem 1.*

Proof Sketch. Since the cost function in Problem 1 is Lipschitz continuous in the state and control space, by Lemma 1, the cost function in the belief space under the 2-Wasserstein metric is also Lipschitz continuous. For belief- \mathcal{A} , the control space, method to sample controls and node selection procedure remains the same as \mathcal{A} . Hence, Belief- \mathcal{A} inherits the asymptotic (ϵ -)optimality properties of \mathcal{A} . \square

B. Computational Efficiency

The overall time complexity of the underlying tree search algorithm does not change. However, planning in the belief space increases the computational effort in two ways. Firstly, planning in the belief space changes the dimension of the search space changes the dimension of the search space. Additionally, our extensions change specific subroutines, giving a computation time increase per call.

1) *Search Dimension:* Planning in the belief space changes the dimension of the search space from n state dimensions to $n + n^2$ Gaussian belief dimensions, which leads to a higher dimensionality of search space increases planning time. However, sampling-based tree motion planners scale very well to moderately high dimensions since a relatively sparse set of sampled nodes may be necessary to construct a valid solution plan.

2) *Distance Metric:* The use of the Wasserstein metric for nearest neighbor queries is slower than usual state space metrics. For general belief distributions, the Wasserstein metric has a time complexity of $O(N^3 \log N)$ for N bin histograms. However, since our beliefs are Gaussian distributions, the Wasserstein distance computation in (13) is more efficient, $O(n^3)$. This is higher than typical state space distance computations of $O(n)$. However, since n is fixed and does not grow with the number of iterations, this leads to a bounded computational time increase per iteration.

3) *Sampling in the Belief Space:* Similarly, the time complexity of sampling random $n \times n$ matrix is $O(n)$, and that of QR decomposition is $O(n^3)$. Therefore, we have an overall time complexity for sampling of $O(n^3)$, which is higher than state space sampling of $O(n)$. Although this is more computationally expensive than usual state space sampling, since n is fixed and does not grow with the number of iterations, this also leads to a bounded computational time increase per iteration.

4) *Node Propagation:* Node propagation using the method described in III-B involves simple matrix additions, multiplications, and inversions. Matrix inversions have a time complexity of $O(n^{2.373})$, which is the dominant term in the propagation routine. This is similar to the state space extension routine, of which time complexity is dominated by matrix multiplications with a time complexity of $O(n^{2.372})$. However, there are more operations per node propagation in the belief space than for state space planning, leading to a higher computational cost per call.

5) *Validity Checking:* In the belief space, the computational cost of the validity checking subroutine depends on the method used. If the obstacles are convex, using the validity checking method described in [11], the approximation of integrals for (3) can be computed as deterministic linear constraints very efficiently, albeit with some conservatism.

Empirically, as seen in the experiments, the belief space extension subroutines are reasonably efficient, allowing for fast planning in the belief space. We also compared to other approaches in the literature which solve similar problems in the belief space, in which our method is shown to have superior computational efficiency.

VI. EXPERIMENTS AND RESULTS

A. Time and Path Length Benchmarks

We compare our methodology on two systems, a 2D system with dynamics

$$\dot{x}_k = x_{k-1} + u_{k-1} + w_k, \quad \dot{z}_k = x_k + v_k(x_k),$$

and a second order unicycle system with dynamics

$$\dot{x} = v \cos(\phi), \quad \dot{y} = v \sin(\phi), \quad \dot{\phi} = \omega, \quad \dot{v} = a.$$

We use dynamic feedback linearization to obtain a linearized closed loop model as presented in [33].

We conducted experiments in specific environments that force a trade-off between motion plans that visit measurement regions to localize and those that correspond to shorter path lengths. These environments, depicted in Fig. 1, are

- 1) Non-observable environment with no obstacles and no measurement region.
- 2) Narrow passage environment with a measurement region. Moving straight to the goal will not satisfy the chance constraint.
- 3) Multi mode solution environment. Two main solution paths are available - A larger passageway that allows reaching the goal region without measurements, and a narrow passage that requires a lower uncertainty.

We compared the effect of using the Wasserstein metric (W_2) with the Euclidean metric (l_2), and including belief sampling bias p_{bias} for belief-RRT (B-RRT) and belief-SST (B-SST). We also ran benchmarks against Rapidly-exploring Random Belief Trees (RRBT) [23], a single query RRG-based optimal planner that solves similar problems. For each case, we use $P_{safe} = 0.95$ and the RRT goal bias $p_{goal} = 0.05$. For all experiments, the cost function is path length. All algorithms are implemented on the Open

Algorithm	Environment 1			Environment 2			Environment 3		
	Time (1st)	Cost (1st)	Cost (10s)	Time (1st)	Cost (1st)	Cost (10s)	Time (1st)	Cost (1st)	Cost (10s)
2D System									
RRBT	0.17	113.8	109.8	1.56	216.1	199.2	2.24	146.8	121.2
B-RRT (l_2)	0.003	194.8	192.6	0.024	360.8	341.7	0.009	293.0	292.6
B-RRT (W_2)	0.029	195.7	186.1	0.2	353.7	345.1	0.016	288.6	285.3
B-RRT ($W_2, 0.2 p_{bias}$)	0.029	189.8	185.8	0.071	348.4	340.0	0.016	294.9	293.8
B-SST (l_2)	0.004	163.6	111.8	2.62	259.4	236.1	0.008	264.9	166.9
B-SST (W_2)	0.029	181.3	111.1	0.51	295.2	236	0.043	263.9	157.4
B-SST ($W_2, 0.2 p_{bias}$)	0.027	168	110.2	0.152	304.7	204.9	0.041	263.2	128.6
Linearized Unicycle									
RRBT	0.225	123.9	120	15.4	227.1	222.6	8.95	201.6	199.4
B-RRT (l_2)	0.011	250.0	250.0	0.447	399.4	367.7	0.045	391.9	390.9
B-RRT (W_2)	0.034	247.6	221.0	0.577	286.4	256.3	0.2	341.8	268.3
B-RRT ($W_2, 0.2 p_{bias}$)	0.041	244.8	231.6	0.61	287.0	260.8	0.19	332.5	289.3
B-SST (l_2)	0.013	198.7	138.5	7.08	267.4	237.9	0.035	339.3	177.8
B-SST (W_2)	0.055	190.3	137.2	2.19	277.8	232.1	0.193	347.2	188.7
B-SST ($W_2, 0.2 p_{bias}$)	0.054	193.8	140.4	0.88	274.5	231.1	0.153	316.1	164.4

TABLE I: Benchmark planner performance results. Each entry is the mean of 100 simulations. Quantification of the standard error may be found in Appendix A and is generally significantly less than the variation between rows. The scores within 10% of the best score in each column are bolded.

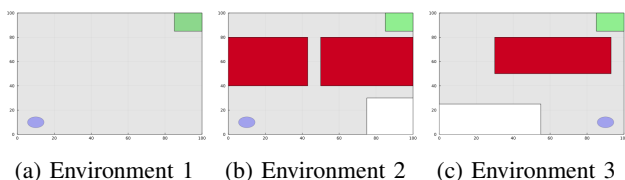


Fig. 1: The initial belief, goal region and obstacles are represented as blue, green and red respectively. White region are measurement regions, in which the measurement noise covariance $R(x_k) = 0.01I$, and with no measurements everywhere else (gray). Environments are 100×100 (m^2).

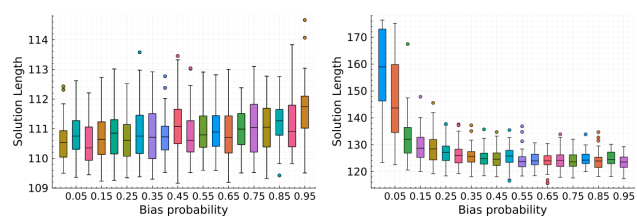
Motion Planning Library (OMPL) [34], and all computations performed single-threaded on a nominally 2.20 GHz CPU.

Table I shows the time taken to compute a first solution, the cost of the first solution, and the solution cost after 10 seconds for each of the environments and dynamics. Belief-SST consistently finds initial solutions very quickly and given additional time, optimizes solutions to low path costs. Using the Euclidean metric instead of the Wasserstein metric computes each iteration faster, but does not find solutions quickly in narrow passageway situations due to the pruning subroutine causing lower uncertainty but higher cost paths to repeatedly be pruned. Belief-RRT finds solutions the fastest but does not improve solutions much when given more time, which is expected as RRT is not asymptotically optimal.

Finally, RRBT computes high quality initial solutions but takes a very long time to do so. This is expected since RRBT exhaustively propagates candidate solutions in the belief space from a state space RRG, so solution paths once found already have low cost. However, RRBT maintains an excessive number of belief nodes for each state RRG vertex that get propagated to a new vertex at each iteration, immensely slowing computation.

B. Sampling Bias

We study the effect of different p_{bias} bias values for the sampling of low uncertainty covariances on solution length and time. The performance of varying bias values with belief-SST is depicted in Fig. 2 (results for Environment 2 are



(a) Environment 1. (b) Environment 3.

Fig. 2: Effect of varying p_{bias} on solution length with 10 seconds of planning time.

similar to that of Environment 3). The bias has a direct effect on the rate of convergence to low solution costs. In Environment 3, a higher p_{bias} leads to faster convergence to better solutions. However, there is a small trade-off in solution cost for Environment 1, in which low uncertainty is not needed. In general, a low value such as $p_{bias} = 0.2$ works well, leading to large gains for environments that require low uncertainty while also performing well in those that do not.

C. Belief-SST with covariance sampling bias

Fig. 3 shows an example of motion plans computed by belief-SST for Environment 3 with the feedback linearized unicycle. Given a short planning time limit, belief-SST quickly finds an initial solution through the larger passageway. As planning time increases, belief-SST improves the solution, converging to one with lower cost by visiting the measurement region before traversing the small passage.

D. Online planning demonstration

Due to the improved speed of computation, our algorithm is able to plan in an online fashion. Fig. 4 shows a simple example showcasing the algorithm's effectiveness in re-planning online when changes to the problem such as new obstacles or measurements are detected. In this example, the robot initially plans with the knowledge that there is one obstacle in red, and finds a motion plan that reaches the goal region. Note that in this plan, there is no need to visit the measurement region since the chance constraint can be satisfied without doing so. However, as the robot moves, it

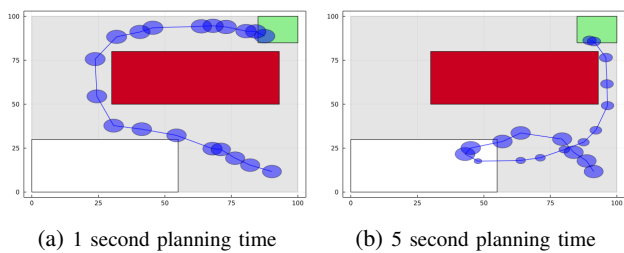


Fig. 3: Runtime results of belief-SST with Wasserstein metric and $p_{bias} = 0.02$, with 2σ Gaussian covariance ellipses.

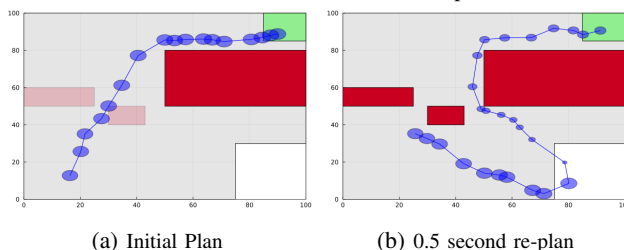


Fig. 4: Online planning scenario. The robot is initially unaware of the obstacles on the left, and plans according to the red obstacle on the right (a). After updating the environment, the robot finds a safe path by localizing at the measurement region in white (b).

updates the environment after detecting obstacles and re-plans. In this updated environment, moving directly to the goal will not satisfy the chance constraint. Therefore, the robot finds a solution plan that moves to the measurement region to localize before traversing safely to the goal region.

VII. CONCLUSION

This paper proposes belief- \mathcal{A} , a general framework for converting any kinodynamical sampling-based tree planner to the belief space for linear systems. The proposed method preserves the convergence properties of the underlying algorithm, and empirical tests demonstrate its efficacy. Future work includes implementing the framework on an actual robotic platform and extending the method to work with a broader class of motion planning algorithms and belief distributions.

REFERENCES

- [1] L. Kavraki, P. Svestka, J.-C. Latombe, and M. Overmars, "Probabilistic roadmaps for path planning in high-dimensional configuration spaces," *IEEE Transactions on Robotics and Automation*, vol. 12, no. 4, pp. 566–580, 1996.
- [2] S. LaValle, "Rapidly-exploring random trees: a new tool for path planning," *The annual research report*, 1998.
- [3] D. Hsu, J.-C. Latombe, and R. Motwani, "Path planning in expansive configuration spaces," in *Proceedings of International Conference on Robotics and Automation*, vol. 3, 1997, pp. 2719–2726 vol.3.
- [4] S. Karaman and E. Frazzoli, "Sampling-based algorithms for optimal motion planning," *International Journal of Robotics Research*, vol. 30, no. 7, pp. 846–894, 2011.
- [5] J. Cortés and T. Siméon, *Sampling-Based Tree Planners (RRT, EST, and Variations)*. Berlin, Heidelberg: Springer Berlin Heidelberg, 2020, pp. 1–9. [Online]. Available: https://doi.org/10.1007/978-3-642-41610-1_170-1
- [6] L. P. Kaelbling, M. L. Littman, and A. R. Cassandra, "Planning and acting in partially observable stochastic domains," *Artificial intelligence*, vol. 101, no. 1-2, pp. 99–134, 1998.
- [7] C. H. Papadimitriou and J. N. Tsitsiklis, "The complexity of Markov decision processes," *Mathematics of Operations Research*, vol. 12, no. 3, pp. 441–450, 1987.
- [8] Z. Sunberg and M. J. Kochenderfer, "Online algorithms for POMDPs with continuous state, action, and observation spaces," in *International Conference on Automated Planning and Scheduling*, 2018.
- [9] N. P. Garg, D. Hsu, and W. S. Lee, "DESPOT- α : Online POMDP planning with large state and observation spaces," in *Robotics: Science and Systems*, 2019.
- [10] B. Luders, M. Kothari, and J. How, "Chance constrained RRT for probabilistic robustness to environmental uncertainty," *AIAA guidance, navigation, and control conference*, 2010.
- [11] L. Blackmore, M. Ono, and B. Williams, "Chance-constrained optimal path planning with obstacles," in *IEEE Trans. on Robotics*, vol. 27, no. 6. IEEE, 2011, pp. 1080–1094.
- [12] È. Pairet, J. D. Hernández, M. Carreras, Y. Petillot, and M. Lahijanian, "Online mapping and motion planning under uncertainty for probabilistically safe autonomous navigation," *IEEE Transactions on Automation Science and Engineering*, 2021.
- [13] E. M. Hahn, V. Hashemi, H. Hermans, M. Lahijanian, and A. Turrini, "Interval markov decision processes with multiple objectives: From robust strategies to pareto curves," *ACM Trans. Model. Comput. Simul.*, vol. 29, no. 4, Nov. 2019. [Online]. Available: <https://doi.org/10.1145/3309683>
- [14] W. Burgard, O. Brock, and C. Stachniss, *The Stochastic Motion Roadmap: A Sampling Framework for Planning with Markov Motion Uncertainty*, 2008, pp. 233–240.
- [15] E. H. Pairet, D. Juan, M. Lahijanian, and M. Carreras, "Motion planning with dynamics by a synergistic combination of layers of planning," *IEEE/RJS International Conference on Intelligent Robots and Systems (IROS)*, pp. 2367–2374, 2018.
- [16] R. Luna, M. Lahijanian, M. Moll, and L. E. Kavraki, "Optimal and efficient stochastic motion planning in partially-known environments," in *The Twenty-Eighth AAAI Conference on Artificial Intelligence*. Quebec City, Canada: AAAI Press, July 2014, pp. 2549–2555. [Online]. Available: <http://www.aaai.org/ocs/index.php/AAAI/AAAI14/paper/view/8457>
- [17] —, "Fast stochastic motion planning with optimality guarantees using local policy reconfiguration," in *IEEE Conference on Robotics and Automation*. Hong Kong, China: IEEE, May 2014, pp. 3013–3019.
- [18] —, "Asymptotically optimal stochastic motion planning with temporal goals," in *Algorithmic Foundations of Robotics XI - Selected Contributions of the Eleventh International Workshop on the Algorithmic Foundations of Robotics, WAFR*, ser. Springer Tracts in Advanced Robotics, vol. 107. Springer, Aug. 2015, pp. 335–352.
- [19] A.-A. Agha-Mohammadi, S. Chakravorty, and N. M. Amato, "FIRM: Sampling-based feedback motion-planning under motion uncertainty and imperfect measurements," *International Journal of Robotics Research*, vol. 33, no. 2, pp. 268–304, 2014.
- [20] T. Shan and B. Englot, "Belief roadmap search: Advances in optimal and efficient planning under uncertainty," in *2017 IEEE/RJS International Conference on Intelligent Robots and Systems (IROS)*, 2017, pp. 5318–5325.
- [21] S. Prentice and N. Roy, "The belief roadmap: Efficient planning in belief space by factoring the covariance," *The International Journal of Robotics Research*, vol. 28, no. 11-12, pp. 1448–1465, 2009. [Online]. Available: <https://doi.org/10.1177/0278364909341659>
- [22] K. L. Platt R, Tedrake R and L.-P. T, "Belief space planning assuming maximum likelihood observations," in *Robotics: Science and Systems*. IEEE, 2010.
- [23] A. Bry and N. Roy, "Rapidly-exploring random belief trees for motion planning under uncertainty," in *Proc. IEEE Int. Conf. on Robotics & Automation*. IEEE, 2011.
- [24] H. Yang, J. Lim, and S. eui Yoon, "Anytime rrtb for handling uncertainty and dynamic objects," in *IEEE/RJS International Conference on Intelligent Robots and Systems (IROS)*. IEEE, 2016.
- [25] Y. Li, Z. Littlefield, and K. E. Bekris, "Asymptotically optimal sampling-based kinodynamic planning," *International Journal of Robotics Research*, vol. 35, no. 5, pp. 528–564, 2016.
- [26] C. Urmon and R. Simmons, "Approaches for heuristically biasing rrt growth," in *Proceedings 2003 IEEE/RJS International Conference on Intelligent Robots and Systems (IROS 2003) (Cat. No.03CH37453)*, vol. 2, 2003, pp. 1178–1183 vol.2.
- [27] M. L. Eaton, "Multivariate statistics: a vector space approach," *Journal of the American Statistical Association*, vol. 80, p. 1069, 1985.
- [28] L. Palmieri and K. Arras, "Distance metric learning for rrt-based mo-

- tion planning with constant-time inference,” *2015 IEEE International Conference on Robotics and Automation (ICRA)*, pp. 637–643, 2015.
- [29] Z. Littlefield, D. Klimenko, H. Kurniawati, and K. Bekris, “The importance of a suitable distance function in belief-space planning,” in *Robotics Research. Springer Proceedings in Advanced Robotics*, vol. 3. Springer, 2018.
- [30] V. M. Panaretos and Y. Zemel, “Statistical aspects of wasserstein distances,” *Annual Review of Statistics and Its Application*, vol. 6, no. 1, pp. 405–431, 2019. [Online]. Available: <https://doi.org/10.1146/annurev-statistics-030718-104938>
- [31] J. Park, C. Park, and D. Manocha, “Efficient probabilistic collision detection for non-convex shapes,” in *Proc. IEEE Int. Conf. on Robotics & Automation*. IEEE, 2017.
- [32] H. Kurniawati and N. M. Patrikalakis, “Point-based policy transformation: Adapting policy to changing pomdp models,” in *Algorithmic Foundations of Robotics X*. Berlin, Heidelberg: Springer Berlin Heidelberg, 2013, pp. 493–509.
- [33] A. De Luca, G. Oriolo, and M. Vendittelli, “Stabilization of the unicycle via dynamic feedback linearization,” *IFAC Proceedings Volumes*, vol. 33, no. 27, pp. 687–692, 2000, 6th IFAC Symposium on Robot Control (SYROCO 2000), Vienna, Austria, 21–23 September 2000. [Online]. Available: <https://www.sciencedirect.com/science/article/pii/S1474667017380114>
- [34] I. A. Şucan, M. Moll, and L. E. Kavraki, “The Open Motion Planning Library,” *IEEE Robotics & Automation Magazine*, vol. 19, no. 4, pp. 72–82, December 2012, <https://ompl.kavrakilab.org>.

APPENDIX

A. Benchmarking Results

Algorithm	Environment 1			Environment 2			Environment 3		
	Time (1st)	cost (1st)	Cost (10 s)	Time (1st)	Cost (1st)	Cost (10 s)	Time (1st)	Cost (1st)	Cost (10 s)
2D System									
RRBT	0.17 ± 0.016	113.8 ± 0.23	109.8 ± 0.032	1.56 ± 0.116	216.08 ± 0.811	199.17 ± 0.626	2.24 ± 0.11	146.8 ± 0.221	121.2 ± 0.437
B-RRT (l_2)	0.003 ± 0.0002	194.8 ± 3.91	192.6 ± 3.51	0.024 ± 0.002	360.75 ± 4.57	341.72 ± 4.336	0.009 ± 0.0008	293.04 ± 4.76	292.61 ± 3.76
B-RRT (W_2)	0.029 ± 0.053	195.7 ± 3.60	186.1 ± 3.62	0.2 ± 0.011	353.7 ± 5.66	345.1 ± 3.96	0.016 ± 0.0009	288.6 ± 3.65	285.3 ± 4.09
B-RRT ($W_2, 0.2 p_{bias}$)	0.029 ± 0.006	189.8 ± 4.09	185.8 ± 3.05	0.071 ± 0.0036	348.4 ± 4.05	340.0 ± 4.27	0.016 ± 0.0008	294.93 ± 3.68	293.81 ± 3.51
B-SST (l_2)	0.004 ± 0.0003	163.6 ± 3.24	111.8 ± 0.124	2.62 ± 0.38	259.4 ± 2.95	236.09 ± 2.83	0.008 ± 0.0008	264.94 ± 4.82	166.85 ± 0.88
B-SST (W_2)	0.029 ± 0.0048	181.3 ± 3.83	111.1 ± 0.13	0.51 ± 0.05	295.2 ± 4.17	236 ± 2.79	0.043 ± 0.0038	263.9 ± 2.94	157.4 ± 1.56
B-SST ($W_2, 0.2 p_{bias}$)	0.027 ± 0.0003	168 ± 3.23	110.2 ± 0.143	0.152 ± 0.01	304.72 ± 3.76	204.87 ± 0.833	0.041 ± 0.0036	263.16 ± 3.42	128.62 ± 0.631
Linearized Unicycle									
RRBT	0.225 ± 0.019	123.9 ± 0.218	120 ± 0.042	15.4 ± 1.08	227.1 ± 0.84	222.6 ± 0.34	8.95 ± 0.563	201.6 ± 1.88	199.4 ± 1.73
B-RRT (l_2)	0.011 ± 0.001	250 ± 6.64	250 ± 7.22	0.447 ± 0.0334	399.4 ± 7.22	367.7 ± 5.83	0.045 ± 0.003	391.9 ± 8.21	390.9 ± 8.1
B-RRT (W_2)	0.034 ± 0.004	247.6 ± 4.13	221 ± 3.88	0.577 ± 0.0468	286.4 ± 7.51	256.3 ± 6.85	0.2 ± 0.015	341.8 ± 6.23	268.3 ± 9.9
B-RRT ($W_2, 0.2 p_{bias}$)	0.041 ± 0.004	244.8 ± 3.49	231.6 ± 4.21	0.61 ± 0.048	287 ± 8.93	260.8 ± 7.73	0.19 ± 0.017	332.5 ± 6.64	289.3 ± 8.46
B-SST (l_2)	0.013 ± 0.001	198.7 ± 4.44	138.5 ± 1.46	7.08 ± 0.69	267.4 ± 3.02	237.9 ± 3.02	0.035 ± 0.0037	339.3 ± 6.62	177.8 ± 5.09
B-SST (W_2)	0.055 ± 0.0048	190.3 ± 4.14	137.2 ± 1.27	2.19 ± 0.242	277.8 ± 4.02	232.1 ± 2.07	0.193 ± 0.014	347.2 ± 6.2	188.7 ± 3.5
B-SST ($W_2, 0.2 p_{bias}$)	0.054 ± 0.0053	193.8 ± 4.52	140.4 ± 1.52	0.88 ± 0.11	274.5 ± 4.60	231.1 ± 2.44	0.153 ± 0.0148	316.1 ± 5.81	164.4 ± 1.52

TABLE II: Benchmark planner performance results. Each entry is the mean of 100 simulations, with standard error of the mean bounds. The scores within 10% of the best score in each column are bolded.